Sivakumar S. K. Tadikonda[1]
Visiting Professor.
Assoc. Mem. ASME

Haim Baruh
Associate Professor.

Department of Mechanical
and Aerospace Engineering,
Rutgers University,
New Brunswick, NJ 08903

Dynamics and Control of a Translating Flexible Beam With a Prismatic Joint

The complete dynamic model of a translating flexible beam, with a tip mass at one end and emerging from or retracting into a rigid base at the other, is presented. The model considers the effect of elastic and translational motions of the beam on each other. The properties of the eigenfunctions of a fixed-free beam are exploited to obtain closed-form expressions for several domain integrals that arise in the model. It is shown that neglecting the effect of elastic motion on the rigid body motion leads to inaccuracies in positioning control. Issues associated with the feedback control of such a beam are discussed.

1 Introduction

Modeling issues associated with flexible links in translational motion and with a prismatic joint at one end have been receiving attention lately. It is usually assumed that translating flexible links can be modeled as beams in flexure with fixed-free end conditions [1-5]. Tabarrok et al. [1] presented certain properties of the mode shapes of fixed-free beams in flexure, as the beam length varies, and these properties are often exploited in deriving the dynamic models for systems containing translating flexible links. The dynamic model of a manipulator consisting of a translating flexible link was presented in [2, 3] that considered the spatial variation of the trial functions, and a similar approach was pursued earlier in [5] for modeling the deployment of the SAFE extension mast from a spacecraft. A lumped mass formulation of an emerging/retracting beam from a rotating base is proposed in [6]. A recent approach in [7] presents a continuum model for a problem similar to that in [6]. However, the model in [7] does not reduce to that in [1] for the no spin case and when fixed-free eigenfunctions are used in the assumed modes method.

The effect of flexible motion on the translational motion of the link was not studied in the above investigations. All these approaches are limited to the case where the translational velocity and acceleration are prescribed *a priori*. While rigid body motion was considered prescribed in the past, recent research [8, 9] indicates a growing interest in investigating the effect of elastic motion on the rigid body motion. It is especially important in the area of robotics where an accurate dynamic model is important for closed-loop control. It will be shown here that neglecting the effect of elastic motion on the translational motion of a link results in pointing inaccuracies in manipulators.

Consider the mechanism shown in Fig. 1. It consists of a rigid support and a flexible link that slides in and out of the support. We assume that the beam was uniform mass and stiffness properties and denote the translational velocity of the beam by $\dot{L}$. It is clear that at any instant, a part of the beam is outside the rigid support and is free to vibrate, while the remaining part of the beam is inside the support and is restrained from vibrating. As the beam is extended (positive $\dot{L}$ in Fig. 1), the length of the vibrating section of the beam increases, while that held inside the rigid support is reduced (vice versa if the beam is retracted); but the total length of the beam remains constant.

We denote the total length of the beam by L_f and the length of the beam outside the support by L and assign the spatial variable x to denote the material point on the outside part of the beam. Let $x=0$ and $x=L$ correspond to the fixed and free ends, respectively. Now, the part of the mean outside the support can be modeled as a fixed-free beam at any time instant. The flexibility in the beam is described by the Euler-Bernoulli model.

2 Properties of the Eigenfunctions of a Fixed-Free Beam

The boundary value problem associated with a uniform beam with an end mass is defined by

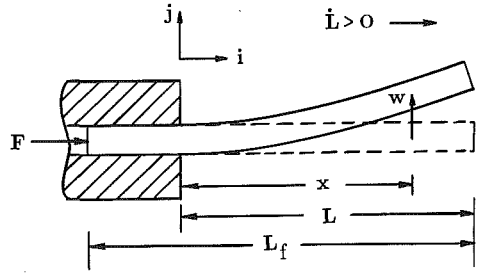

Fig. 1 A beam with a prismatic end condition

[1]Currently, DYNACS Engineering Co., Palm Harbor, FL.

Contributed by the Dynamic Systems and Control Division for publication in the JOURNAL OF DYNAMIC SYSTEMS, MEASUREMENT, AND CONTROL. Manuscript received by the Dynamic Systems and Control Division January 9, 1990; revised manuscript received August 28, 1991. Associate Technical Editor: A. G. Ulsoy.

$$EIu''''(x) - \lambda\rho u(x) = 0 \tag{1}$$

with the associated boundary conditions

$$u(0) = u'(0) = 0$$
$$EIu''(L) = 0$$
$$EIu'''(L) = -M_e\omega^2 u(L) \tag{2}$$

where, EI and ρ are the stiffness and mass per unit length, respectively, M_e is the end mass, and $u(x)$ is the elastic displacement of a point along the beam with spatial coordinate x. Primes denote differentiation with respect to x.

By solving the eigenvalue problem, the characteristic equation is obtained as

$$1 + \cos\beta L \cosh\beta L = \frac{\lambda M_e}{\rho L}(\sin\beta L \cosh\beta L - \cos\beta L \sinh\beta L) \tag{3}$$

and the eigenfunctions associated with each of the solutions of the characteristic equation are given by

$$\phi_e(x, L) = C_r[(\cos\beta_r x - \cosh\beta_r x) + A_r(\sin\beta_r x - \sinh\beta_r x)] \tag{4}$$

where,

$$\beta^4 = \frac{\lambda\rho}{EI}, \tag{5}$$

$$A_r = \frac{\sin\beta_r L - \sinh\beta_r L}{\cos\beta_r L + \cosh\beta_r L} \tag{6}$$

and C_r's are the normalization constants obtained from

$$\int_0^L \phi_i\phi_j\rho dx + M_e\phi_i(L)\phi_j(L) = \delta_{ij} \tag{7}$$

where, δ_{ij} is the Kronecker delta. The natural frequencies are obtained from the relation $\omega^2 = \lambda$.

If such a system is under deployment, i.e., a flexible beam is used to deploy a satellite or a payload, the length of the flexible beam will be changing at the deployment rate. The frequencies of the beam also undergo a continuous change. This can be seen by differentiating the characteristic equation, Eq. (3), with respect to the instantaneous length L of the beam to obtain

$$\frac{d\lambda}{dL}\left(\left(1 + \frac{M_e}{\rho L}\right) + \frac{\lambda M_e}{\rho L}\frac{2\sin\beta L \sinh\beta L}{(\sin\beta L \cosh\beta L - \cos\beta L \sinh\beta L)}\right) = \frac{\lambda M_e}{\rho L^2} \tag{8}$$

It can be seen that the rate of change of the eigenvalues of the beam is dependent on the instantaneous beam length L. The same conclusions can be drawn for the mode shapes, Eq. (4). The expression for $d\phi_r(x, L)/dL$ is very complicated and hence it not given here.

If eigenfunctions are used in the expansion of a deploying beam in a multibody dynamics formalism, the time rates of change of the eigenfunctions will be needed as well. However, if the endmass is absent, Eq. (8) becomes

$$\frac{d\lambda}{dL} = \frac{d}{dL}(\beta L) = 0 \tag{9}$$

which implies that the eigenvalues λ are independent of the length L, or the variation of β's and the natural frequencies ω's are given by

$$\frac{d\beta}{dL} = \frac{-\beta}{L} \quad \text{and} \quad \frac{d\omega}{dL} = \frac{-2\omega}{L} \tag{10}$$

A closed-form solution for ω is given by

$$\omega(L) = D/L^2 \tag{11}$$

where the length dependency of the frequencies is stated explicitly and $D = \omega(L_0)L_0^2$ is a constant. It can then be shown, for such beams, that the normalization constants $C_r = 1/\sqrt{\rho L}$ for all the eigenfunctions, and also that

$$\frac{d\phi_r(x, L)}{dL} = \frac{-1}{2L}\phi_r(x, L) - \frac{x}{L}\frac{d\phi_r(x, L)}{dx} \tag{12}$$

where, the length L on the right side of Eq. (4) is also treated as a variable in obtaining the above result. Because of the simplicity of the eigenfunctions of a fixed-free beam with no end mass, and the associated properties given by Eqs. (9–12), the use of these functions as admissible function is more attractive than using the exact eigenfunctions in an assumed mode expansion for flexible beams deploying payloads. This is because these trial functions display the length-varying properties, and their use results in a set of equations that is an order of magnitude less complex than the equations with the exact eigenfunctions. Hence, the eigenfunctions of a fixed-free beam (Eq. (4) with $C_r = 1/\sqrt{\rho L}$) will be used as the trial functions in the derivation of the dynamics as described in the next section.

3 Equations of Motion

Consider a beam moving longitudinally with a velocity of $\dot{L}$, with one end free and the other end connected to the base with a prismatic joint, as shown in Fig. 1. Denote the elastic displacement of a point A along the beam by $u(x, L, t)$, where the dependency on the length is made explicit and the material point is defined with respect to the (instantaneous) fixed end. Then, $x = 0$ and $x = L$ correspond to the fixed and free ends, respectively. The total displacement of a material point A with respect to the fixed-end then has the form[2]

$$\mathbf{r} = (x + w(x, L, t))\mathbf{i} + u(x, L, t)\mathbf{j} \tag{13}$$

where $w(x, L, t)$ describes the shortening of the projection [8]. Assuming that the vibration in the longitudinal direction is negligible, $w(x, L, t)$ has the form

$$w(x, L, t) \approx -\frac{1}{2}\int_0^x (u'(\zeta, L, t))^2 d\zeta \tag{14}$$

The absolute velocity $\dot{\mathbf{r}}$ of the material point with respect to an inertial frame is:

$$\dot{\mathbf{r}} = \dot{L}\mathbf{i} + \dot{w}(x, L, t)\mathbf{i} + \dot{u}(x, L, t)\mathbf{j} \tag{15}$$

The kinetic energy can be obtained as

$$KE = \frac{1}{2}\int \dot{\mathbf{r}}\cdot\dot{\mathbf{r}}\, dm = \frac{1}{2}(m + M_e)\dot{L}^2 + \frac{1}{3}\int_0^L \rho_{eff}(\dot{w}^2(x, L, t) + 2\dot{L}\dot{w}(x, L, t) + \dot{u}^2(x, L, t))dx \tag{16}$$

where L_f is the total length of the beam, ρ is the mass per unit length of the beam, $m = \rho L_f$ is the beam total mass, M_e is the endmass and $\rho_{eff} = \rho + M_e\delta(x - L)$, where δ represents the Dirac-delta function.

Using the method of assumed modes, the displacement can be expressed in terms of the instantaneous eigenfunctions of a fixed-free beam, given by Eq. (4), as

$$u(x, L, t) = \sum_{r=1}^{N}\phi_r(x, L)u_r(t) \tag{17}$$

where $u_r(t)$ are the time-dependent amplitudes and N is the number of terms retained in the expansion. The shortening of projection then has the form

$$w(x, L, t) = -\frac{1}{2}\sum_{i=1}^{N}\sum_{j=1}^{N}\int_0^x \phi_i'(\zeta, L)\phi_j'(\zeta, L)d\zeta u_i(t)u_j(t). \tag{18}$$

[2] Bold characters denote vectors and **i** and **j** are the unit vectors.

The time rate of change of the elastic displacement can be obtained by differentiating Eq. (17) with respect to time as

$$\dot{u}(x, L, t) = \sum_{r=1}^{N} \left(\frac{d}{dt} (\phi_r(x, L)) u_r(t) + \phi_r(x, L) \dot{u}_r(t) \right). \quad (19)$$

Note that $\dot{u}(x, L, t)$ represents the velocity of a material point at a distance $(L-x)$ from the free end. The expression for d/dt $(\phi_r(x, L))$ then is

$$\frac{d}{dt} (\phi_r(x, L)) = -\frac{\dot{L}}{2L} \phi_r(x, L) + \frac{\dot{L}}{L} (L-x) \phi_r'(x, L). \quad (20)$$

The expansion in Eq. (19) can be used to obtain the time rate of change of foreshortening, which, along with Eq. (20), can then be substituted into Eq. (16) to obtain the kinetic energy. Since $w(x, L, t)$ contains terms quadratic in $u_r(t)$, $\dot{w}^2(x, L, t)$ contains higher order terms in $u_r(t)$, and assuming that the elastic displacements are small, terms of order higher than quadratic in $u_r(t)$ or $\dot{u}_r(t)$ will be neglected.

At this stage, it is helpful to introduce the following definitions to improve the clarity in further development.

$$M_{rs} = \int_0^L \left(-\frac{1}{2} \phi_r + (L-x) \phi_r' \right) \left(-\frac{1}{2} \phi_s + (L-x) \phi_s' \right) \rho_{eff} dx$$
$$= \hat{M}_{rs} + \frac{M_e}{4} \phi_r(L) \phi_s(L) \quad (21)$$

$$N_{rs} = \int_0^L \phi_r \left(-\frac{1}{2} \phi_s + (L-x) \phi_s' \right) \rho_{eff} dx$$
$$= \hat{N}_{rs} - \frac{M_e}{2} \phi_r(L) \phi_s(L) \quad (22)$$

$$S_{rs} = L \int_0^L \rho_{eff} (L-x) \phi_r' \phi_s' dx$$
$$= \hat{S}_{rs} \quad (23)$$

The terms independent of the endmass are represented by a hat ($\hat{()}$) in the above equations. At the outset, it may appear that these integrations must be carried out for all possible lengths of the beam. However, it can be shown [1] that the matrices $\hat{M}$, $\hat{N}$, and $\hat{S}$ are constants are are independent of the length L, mass density and stiffness (if they are not functions of x), and if the eigenfunctions are normalized according to Eq. (7), for fixed-free beam eigenfunctions. Hence,

$$\frac{d\hat{M}_{rs}}{dL} = \frac{d\hat{N}_{rs}}{dL} = \frac{d\hat{S}_{rs}}{dL} = 0. \quad (24)$$

In addition, the values of the eigenfunctions at the tip are given by

$$\phi_r(L) = \frac{2}{\sqrt{\rho L}} (-1)^{r+1} \quad (25)$$

Thus, no additional domain integrations need to be performed at each time step during either control or simulation. The matrices $\hat{M}$, $\hat{N}$, and $\hat{S}$ are tabulated in [7] for a uniform beam.

Substituting Eq. (25) into Eqs. (19)–(23) and the result into Eq. (16) the kinetic energy can be obtained as

$$KE = \frac{1}{2} (m + M_e) \dot{L}^2 + \frac{1}{2} \sum\sum \left(\delta_{ij} + \frac{4M_e}{\rho L} (-1)^{i+j} \right) \dot{u}_i \dot{u}_j$$
$$+ \frac{\dot{L}^2}{2L^2} \sum\sum (M_{ij} + S_{ij}) u_i u_j + \frac{\dot{L}}{L} \sum\sum (N_{ji} - S_{ij}) u_i \dot{u}_j \quad (26)$$

The potential energy is given by

$$PE = \frac{1}{2} \int_0^L EI (u'')^2 dx \quad (27)$$

Note that the ω's correspond to the instantaneous length of the beam. Substituting Eq. (17) in Eq. (27), we obtain

$$PE = \frac{1}{2} \sum_r \omega_r^2 u_r^2 \quad (28)$$

Using Eq. (11) in Eq. (28) we obtain

$$PE = \frac{1}{2L^4} \sum_r D_r^2 u_r^2. \quad (29)$$

The Lagrangian $\mathcal{L}$ is formed as

$$\mathcal{L} = KE - PE \quad (30)$$

The equations of motion can be obtained in the standard form using Lagrange's equations. The independent variables are: the beam length L, and the modal amplitudes u_1, u_2, ..., u_N.

Assuming that control force for the rigid-body motion manipulation of the beam is provided inside the "built-in" end as shown in Fig. 1, the virtual work is obtained as:

$$\delta W = F \delta L \quad (31)$$

where δ represents the variation, and F is the control force.

Using Eqs. (26), (29) and (24), and the Lagrange's equations, the equations of motion are obtained as

$$\left[m + M_e + \frac{1}{L^2} \sum_{i=1}^{N} \sum_{j=1}^{N} \left(\hat{M}_{ij} + \hat{S}_{ij} + \frac{M_e}{\rho L} (-1)^{i+j} \right) u_i u_j \right] \ddot{L}$$
$$+ \frac{1}{L} \sum_{i=1}^{N} \sum_{j=1}^{N} \left[\hat{N}_{ji} - \hat{S}_{ij} - \frac{2M_e}{\rho L} (-1)^{i+j} \right] u_i \ddot{u}_j$$
$$- \frac{\dot{L}^2}{L^3} \sum_{i=1}^{N} \sum_{j=1}^{N} \left[\hat{M}_{ij} + \hat{S}_{ij} + \frac{3M_e}{2\rho L} (-1)^{i+j} \right] u_i u_j$$
$$+ \frac{2\dot{L}}{L^2} \sum_{i=1}^{N} \sum_{j=1}^{N} \left[\hat{M}_{ij} + \hat{S}_{ij} + \frac{M_e}{\rho L} (-1)^{i+j} \right] u_i \dot{u}_j$$
$$- \frac{1}{L} \sum_{i=1}^{N} \sum_{j=1}^{N} S_{ij} \dot{u}_i \dot{u}_j - \frac{2}{L} \sum_{i=1}^{N} \frac{D_i^2}{L^4} u_i^2 = F \quad (32)$$

for the translational motion of the beam, and

$$\sum_{j=1}^{N} \left[\delta_{rj} + \frac{4M_e}{\rho L} (-1)^{r+j} \right] \ddot{u}_j + \frac{\ddot{L}}{L} \sum_{i=1}^{N} \left[\hat{N}_{ri} - \hat{S}_{ri} \right.$$
$$\left. - \frac{2M_e}{\rho L} (-1)^{r+i} \right] u_i - \frac{\dot{L}^2}{L^2} \sum_{i=1}^{N} \left[\hat{N}_{ri} + \hat{M}_{ri} - \frac{3M_e}{\rho L} (-1)^{r+i} \right] u_i$$
$$+ 2 \frac{\dot{L}}{L} \sum_{i=1}^{N} \left[\hat{N}_{ri} - \frac{2M_e}{\rho L} (-1)^{r+i} \right] \dot{u}_i + \frac{D_r^2}{L^4} u_r = 0,$$
$$r = 1, 2 \ldots N \quad (33)$$

for the flexible motion coordinates. Note that Eq. (33) agrees with the elastic motion equations in [1] in the absence of an end mass.

It can be observed that it is important to include the geometric stiffening effect in the dynamics, because its contribution, as indicated by the S_{ij} terms, is of the same order as M_{ij} that is due to the coupling between the deployment and vibrational motions.

Equations (32) and (33) represent a set of coupled nonlinear equations. These equations clearly demonstrate the effects of elastic and translational motions on each other. It can be seen that no domain integrations need to be performed to evaluate these terms, no eigenvalue problem needs to be solved as the length varies and that the dynamic model does not contain any time-varying coefficients.

Note that the dynamics of a telescopic boom can be similarly formulated with the mass and stiffness densities ρ and EI replaced by $\rho(x, L)$ and $EI(x, L)$, respectively. The equations of motion will be more complicated because the variation of integrals in Eqs. (21)–(23) with respect to the length L must

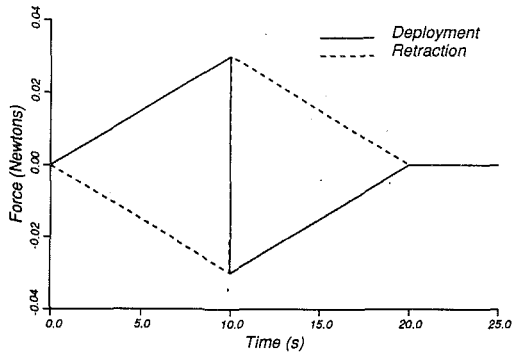

Fig. 2 An open-loop force profile

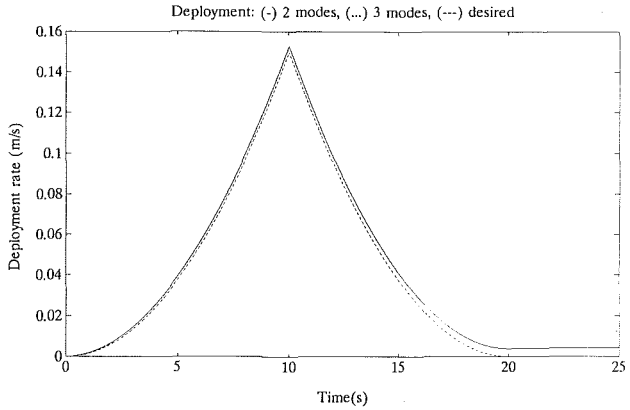

Fig. 3 Translational velocity during during deployment, $N=2$ and $N=3$

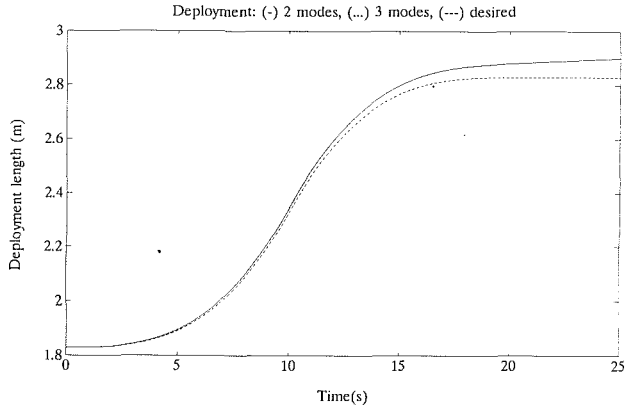

Fig. 4 Length of the vibrating beam during deployment, for $N=2$ and $N=3$

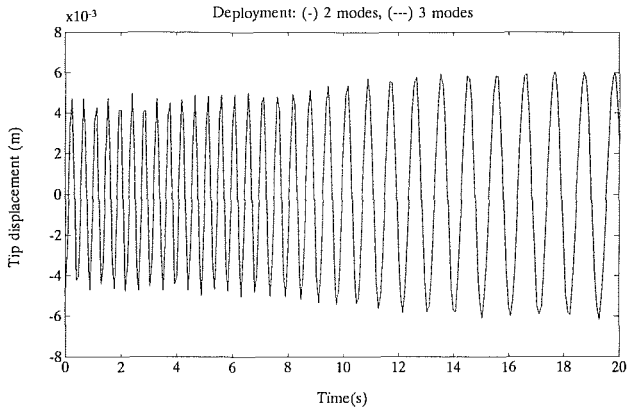

Fig. 5 Tip deflection as a function of time, during deployment

now consider an additional term that corresponds to $d\rho(x, L)/dL$ and the derivaties of kinetic and potential energies will contain the terms $d\rho(x, L)/dL$ and $dEI(x, L)/dL$. Explicit expressions for $\rho(x, L)$ and $EI(x, L)$ will be required if the evaluation of domain integrations at each time step is to be avoided when solving the equations of motion.

4 Numerical Example

We consider a uniform beam whose dimensions are the same as in [8]. It is 3.657 meters (12 ft) long ($L_f=3.657$ m) and has a 15.24×0.952 cm ($6\times3/8$ in) cross section. The unit mass and stiffness are $\rho=4.015$ kg/m (5.823×10^{-4} lb.s^2/in^2) and $EI=756.65$ N/m^2 (263672 lb.in^2), respectively. Its transverse vibration in the thickness direction is of interest. The first three solutions of the characteristic equation are: $\beta L=1.875105$, 4.694092, and 7.854758. We investigate the deployment and retraction maneuvers with and without feedback control.

4.1 Deployment and Retraction Without Feedback Control. We first consider the case of beam deployment ($L>0$) with no endmass. The deployment specification is that the beam be extended exactly 1.0 m in 20.0 s and that there be no translational motion after the deployment. An open-loop control can be easily realized so that these requirements are met. Such a force profile is shown in Fig. 2. The initial length of the vibrating section of the beam is $L(0)=L_f/2=1.8288$ m, and $\dot{L}(0)=0$ at $t=0$. The first three natural frequencies of such a beam for $L=1.8288$ m are: 14.4326, 90.4476, and 253.2557 rad/s. It was reported in [10] that initial tip displacement strongly demonstrated the coupling between the elastic and rigid-body motions. Hence, we consider the deployment with an initial tip displacement of $\bar{\delta}=5$ mm. The elastic curve of the beam can be obtained from statics as

$$\psi(x)=-\bar{\delta}x^2(3L-x)/2L^3,\quad 0<x<L \tag{34}$$

The initial values for the amplitudes $u_r(t)$ can be obtained from

$$u_r(0)=(\psi(x),\ \phi_r(x))=\int_0^L \rho\psi(x)\phi_r(x)dx \tag{35}$$

The tip is then released. The initial energy in the system is solely due to the elastic motion, and is calculated from

$$E=\frac{1}{2}\sum_{r=1}^{N}[\dot{u}_r^2(0)+\omega_r^2(L(0))u_r^2(0)] \tag{36}$$

as 4.6177×10^{-3} and 4.632×10^{-3} Joules for two and three terms in the modal expansion, respectively. It is not possible to compute the energy in each mode for $t\neq0$ because of the coupling between the elastic and rigid-body motions. The translational velocity, the instantaneous vibrating length of the beam, and the tip displacement are shown in Figs. 3, 4, and 5, respectively, for $N=2$ and 3. It can be seen that two modes are sufficient to represent the elastic motion and that the elastic motion has a significant effect on the translational motion of the beam. The transfer of energy between modes does not appear to be as significant as that of the transfer from the elastic motion to the translational motion. Also plotted in Figs. 3 and 4 are the counterparts in the absence of the effect of elastic motion on the rigid-body motion.

The total energy after the open-loop maneuver is 1.972×10^{-3} Joules and it is the same for both the $N=2$ and $N=3$ cases. The first three frequencies of the beam for $L=2.9006$ m (for $N=3$ and at $t=25$ s) are: 5.737, 35.953, and 100.67 rad/s.

Next we consider the case of retraction of the beam ($L<0$), also with the endmass. The initial length of $L(0)=L_f$ and $\dot{L}(0)=0$. The first three natural frequencies for $L=L_f$ are: 3.6082, 22.6119, and 63.3139 rad/s. An open-loop force profile is synthesized for the retraction of this beam that, in the absence of elastic effects, results in a retraction of exactly 1.0 m in 20.0 s such that $L(t=25)=0$. This open-loop force profile is

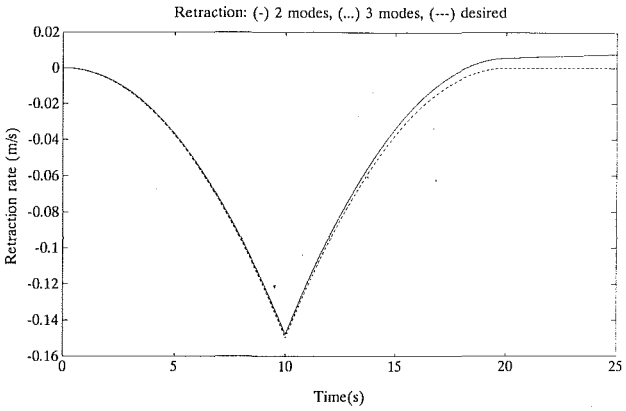

Fig. 6 Translational velocity as a function of time, during retraction

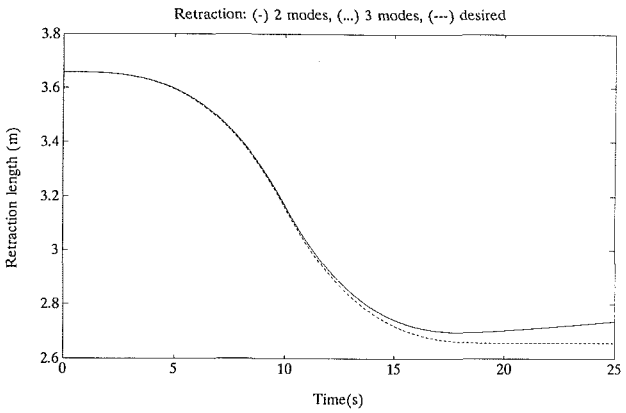

Fig. 7 Length of the vibration beam as a function of time, during retraction

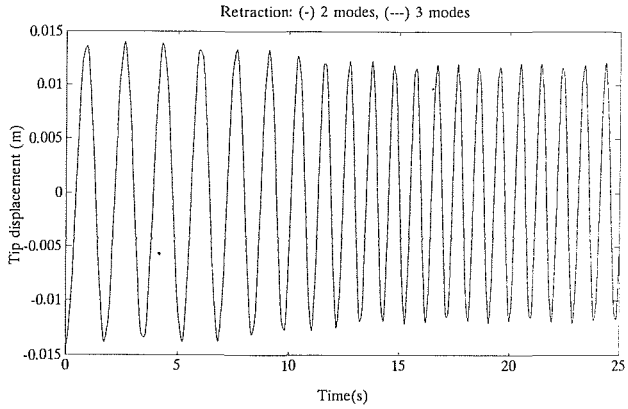

Fig. 8 Tip deflection as a function of time, during retraction

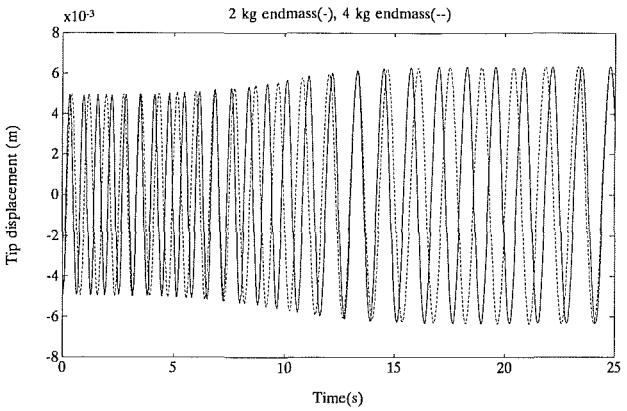

Fig. 9 Tip deflection with an endmass

also shown in Fig. 2. Initial tip deflection is provided as in the previous case, except that $\bar{\delta}=14.142$ mm so that the initial energy in the system is the same as in the deployment case.

The translational velocity L, the length of the vibrating section of the beam and the tip deflection are plotted in Figs. 6, 7, and 8, respectively. The effect of elastic motion on rigid-body motion is once again apparent. The total final energy is 8.695×10^{-3} and 8.706×10^{-3} Joules, for $N=2$ and 3, respectively. The frequencies of the beam at $t=25$ s (for $N=3$) are: 6.442, 40.363 and 113.035 rad/s.

It can be observed from Figs. 3 and 6 that extension time reduced and retraction time increased due to the effect of flexible motion in the translation. This is due to the "pull" exerted by the elastic motion on the translational motion and is always directed away from the fixed end. Hence, the extension velocity increased and the retraction velocity reduced. This fact is even more striking during retraction (Figs. 6 and 7). The translational velocity gradually reduced to zero and then became positive, i.e., the beam starts to move out. In the absence of any active control force, the beam continues to be "pulled" out.

The amplitude of the flexible motion increased during deployment and decreased during retraction. This can be anticipated because the beam becomes "softer" as the length increases and "stiffer" as the length reduces. The increase in the spacing of the oscillations in Fig. 5 and the reduction in the spacing in Fig. 8 can be observed, which are due to the "softening" and "stiffening" of the beam, respectively.

Also, note the difference in the energy levels in extension and retraction after the open-loop control ceased. Although the initial energy levels are the same, the final energy in retraction is higher than that in extension by an order of magnitude. As stated before, the effect of vibration is to increase the translational velocity during extension and reduce it during retraction. Hence, more energy is trapped in the elastic motion during the retraction of the beam.

We next present the case of the deployment of a beam with a tip mass, using the eigenfunctions of a fixed-free beam as the trial functions, for the same deployment profile used in Figs. 3-5. The tip displacement is plotted in Fig. 9, for $M_e=2$ kg and $M_e=4$ kg and with $N=2$ during deployment. It clearly demonstrates that the frequencies reduce as the tip mass increases.

4.2 Feedback Control of Elastic Motion. A simple decentralized control of the elastic motion is now considered. Let the actuator locations be denoted by x_{ai} $(i=1, 2, \ldots, N_a)$, where N_a is the number of actuators. The decentralized control law is of the form [11, 12]

$$F_i=\alpha_i u(x_{ai}, t)+\beta_i \dot{u}(x_{ai}, t) \tag{37}$$

where, α_i and β_i are the feedback gains associated with ith actuator. The modal forces are obtained from

$$f_r=\sum_{i=1}^{N_a}\int F_i\delta(x-x_{ai})\phi_r(x, L)dx \tag{38}$$

Using Eqs. (17-20) in the above, the modal forces can be written as:

$$f_r=\sum_{j=1}^{N}B_{rj}u_j+\sum_{j=1}^{N}C_{rj}\dot{u}_j+\frac{\dot{L}}{L}\sum_{j=1}^{N}D_{rj}u_j \tag{39}$$

where,

$$B_{rj}=\sum_{i=1}^{N_a}\alpha_i\phi_r(x_{ai})\phi_j(x_{ai}),$$

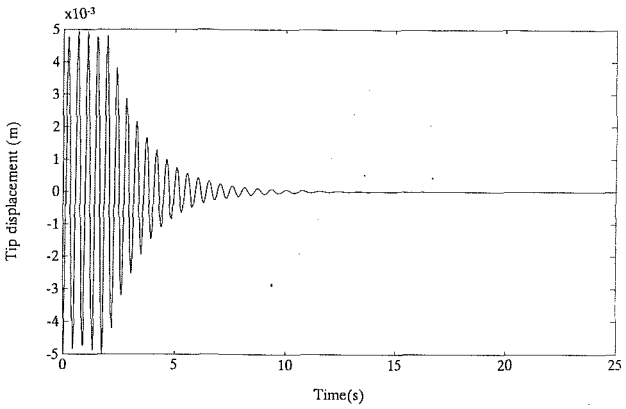

Fig. 10 Feedback control of the elastic motion, during deployment

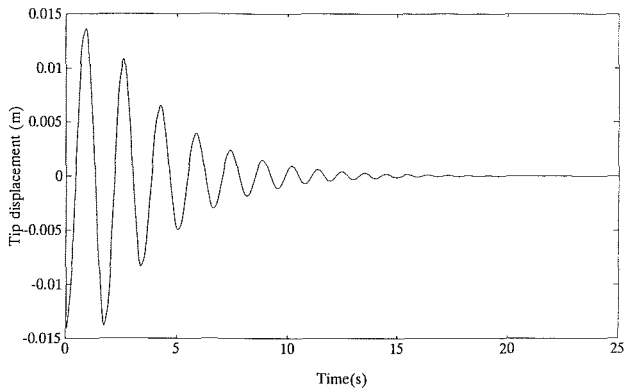

Fig. 11 Feedback control of the elastic motion, during retraction

$$C_{rj} = \sum_{i=1}^{N_a} \beta_i \phi_r(x_{ai}) \phi_j(x_{ai}),$$

$$D_{rj} = \sum_{i=1}^{N_a} \beta_i \phi_r(x_{ai}) \left(-\frac{1}{2} \phi_j(x_{ai}) + (L - x_{ai}) \phi_j'(x_{ai}) \right) \quad (40)$$

Note that if the actuation is through a distributed actuator, the summation in Eq. (40) will be replaced by integration, and if $\alpha_i = \alpha$ and $\beta_i = \beta$, then $B_{rj} = \alpha \delta_{rj}$, $C_{rj} = \beta \delta_{rj}$ and $D_{rj} = \beta N_{rj}$. Also note that *closed-loop poles cannot be evaluated* because of the nonlinear coupling between the elastic and the rigidbody motions.

It should be mentioned that although α_i and β_i may be chosen as constants, B_{rj}, C_{rj} and D_{rj} change continuously. The extension and retraction cases are revisited with this feedback with two actuators located along the beam, one at the tip of the beam and the other at $x = L/2$ at $t = 0$. The initial conditions for these cases are the same as those for the earlier cases and with no endmass. The tip deflection is plotted in Figs. 10 and 11, respectively, for the deployment and retraction cases for $\alpha_i = -1.0$ and $\beta_i = -0.5$ ($i = 1, 2$) and for $N = 2$. The marked improvement is apparent. Note that because the initial energy in the system is required to be the same both during deployment and retraction, and since the beam initial frequencies during retraction are smaller than those during deployment, the tip displacement is correspondingly larger during retraction.

5 Discussion

A complete dynamic model for a translating flexible beam deploying a payload from a fixed base is presented. The model considers the effects of translational and elastic motions on each other. The properties of the eigenfunctions of a uniform fixed-free beam are exploited in the dynamic model. Their use as trial functions for beams carrying a tip mass is shown to eliminate the need to evaluate various domain integrals that arise in the equation of motion, at every time step. The equations of motion for the translational and flexible motions, derived from a Lagrangian analysis, are shown to be nonlinear, coupled and time-varying. However, the time-dependence of various terms is made implicit using the properties of the eigenfunctions.

Although the characteristic of elastic motion (frequencies and eigenfunctions) change as the length varies, it is shown that energy conservation is achieved, in the absence of damping and external forces, by redistribution of the energy between the elastic and translational motions. The amount of energy in the system is used as an indicator for measuring the effect of elastic motion on the translational motion of the beam. Numerical simulations presented show the transfer of energy between elastic and translational motions to be more significant than that between the various modes. It is demonstrated that the effect of elastic motion on the translational motion is significant and cannot be neglected when trajectory tracking or accurate positioning of the end is desired.

The length-varying nature of the eigenfunctions is considered in a decentralized control law investigated for controlling the elastic motion. The deployment is achieved through open-loop control. The closed-loop poles cannot be obtained for this system.

Acknowledgment

The authors would like to thank an anonymous reviewer for his/her critical comments and helpful suggestions.

References

1 Tabarrok, B., Leech, C. M., and Kim, Y. I., "On the Dynamics of an Axially Moving Beam," *Journal of the Franklin Institute*, Vol. 297(3), Mar. 1974, pp. 201-220.

2 Wang, P. K. C., and Wei, J. D., "Vibrations in a Moving Flexible Robot Arm," *Journal of Sound and Vibration*, Vol. 116(1), 1987, pp. 149-160.

3 Krishnamurthy, K., "Dynamic Modelling of a Flexible Cylindrical Manipulator," *Journal of Sound and Vibration*, Vol. 132(1), June 1989, pp. 143-154.

4 Chalhoub, N. G., and Ulsoy, A. G., "Dynamic Simulation of a Flexible Arm and Controller," ASME JOURNAL OF DYNAMIC SYSTEMS, MEASUREMENT AND CONTROL, Vol. 108, June 1986, pp. 119-126.

5 Weeks, G. E., "Dynamic Analysis of a Deployable Space Structure," *Journal of Spacecraft and Rockets*, Vol. 23(1), Jan.-Feb. 1986, pp. 102-107.

6 Banerjee, A. K., and Kane, T. R., "Extrusion of a Beam from a Rotating Base," *Journal of Guidance, Control and Dyanmics*, Vol. 12(2), Mar.-Apr. 1989, pp. 140-146.

7 Yuh, J., and Young, T., and "Dynamic Modeling of an Axially Moving Beam in Rotation: Simulation and Experiment," ASME JOURNAL OF DYNAMIC SYSTEMS, MEASUREMENT, AND CONTROL, Vol. 113, Mar. 1991, pp. 34-40.

8 Baruh, H., and Tadikonda, S. S. K., "Issues in the Dynamics and Control of Flexible Robot Manipulators," *Journal of Guidance, Control and Dynamics*, Vol. 12(5), Sept.-Oct. 1989, pp. 659-671.

9 Nagarajan, S., and Turcic, D. A., "Langrangian Formulation of the Equations of Motion for Elastic Mechanisms with Mutual Dependence between Rigid Body and Elastic Motions: Parts I & II," ASME JOURNAL OF DYNAMIC SYSTEMS, MEASUREMENT AND CONTROL, Vol. 112, pp. 203-224, June 1990.

10 Lips, K. W., and Modi, V. J., "Three-Dimensional Response Characteristics for Spacecraft with Deploying Flexible Appendages," *Journal of Guidance, Control and Dynamics*, Vol. 4(6), Nov.-Dec. 1981, pp. 650-656.

11 Silverberg, L. M., "Uniform Damping Control of Spacecraft," *Journal of Guidance, Control and Dynamics*, Vol. 9, 1986, pp. 221-227.

12 Aubrun, J. N., "Theory of Structures with Low Authority Controllers," *Journal of Guidance, Control and Dynamics*, Vol. 3, 190, pp. 444-451.